

# Experimental modal analysis of SSR1 cryomodule for numerical model tuning and validation

A Barnaba<sup>1</sup>, F Bucchi<sup>1</sup>, P Neri<sup>1,\*</sup> and D Passarelli<sup>2</sup>

<sup>1</sup>University of Pisa, Department of Civil and Industrial Engineering, largo L. Lazzarino 1, 56122 Pisa, Italy

<sup>2</sup>Fermilab, Batavia, IL, USA

E-mail: [a.barnaba@studenti.unipi.it](mailto:a.barnaba@studenti.unipi.it)

[francesco.bucchi@unipi.it](mailto:francesco.bucchi@unipi.it)

[paolo.neri@dici.unipi.it](mailto:paolo.neri@dici.unipi.it)

[donato@fnal.gov](mailto:donato@fnal.gov)

**Abstract.** The present activity aims to test the Cryomodule SSR1 to validate the corresponding mixed multibody-finite element numerical model and to determine the range of frequencies in which the first natural modes of the structure lie. The experimental activity consisted of a hammer test of the cryomodule at an early assembly stage at which the internal parts, constituting the cold mass, are accessible and, thus, many accelerometers can be attached to the beam string. The comparison between the experimental results obtained for the sub-assembly and the numerical results obtained for the corresponding sub-model, derived from the previously developed complete model, allowed to assess the validity of the numerical model and to get feedback on the effectiveness of the placement of the sensors in capturing the dynamic response of the system during transportation.

## 1. Introduction

In the framework of the PIP-II project for the upgrade of Fermilab's particle accelerator complex, a major role is played by the transportation of the different components that constitute the cryomodules. A cryomodule is a structure that consists of one string of metallic vacuum-sealed chambers, the so-called Superconducting Radio Frequency (SRF) cavities [1], which act as propellers for the particle beam that is continuously accelerated through the cavities, using an electromagnetic field generated by superconducting materials [2] at cryogenic temperatures in a vacuum environment [3]. The PIP-II project exploits different types of cavities: 325 MHz single spoke resonators (SSR1, SSR2) [4], half wave resonator (HWR) [5, 6], and 650 MHz multicell cavities (LB650, HB650) [7]. During the fabrication and the assembly process, the cryomodules are transferred to different sites and to their final location where several cryomodules are assembled in a queue to form a long beamline, which is at the very heart of the superconducting linear accelerator. The transportation phase of the cavity string and its secondary components has proved to be challenging [8, 9]. Several parts and joints that compose the cryomodule are very fragile and their airtightness must be ensured during the whole lifecycle of the cryomodule. In this perspective, the dynamic loads caused by the road asperities during the

---

\* Corresponding author

transportation may seriously compromise the functionality of the assemblies being transported. To design an effective system to dampen and reduce the acceleration experienced by the cryomodule, the first step consists in the development of a numerical model to study and investigate different approaches and technical solutions capable of acting as mechanical filters against the loading coming from the truck bed used for the transport. Since these are large models that need many severe hypotheses to shorten the computational time, their experimental validation is of utmost importance. The present paper aims to discuss the results obtained by an experimental modal analysis performed on a sub-assembly of the Cryomodule SSR1 to validate the developed numerical model, a combination between finite element and multibody modelling (a strategy already developed by the authors in [10]), and to determine the range of frequencies in which the first natural modes of the structure lie. A full description of the numerical model can be found in [11].

To validate numerical models, experimental modal analysis [12], as well as experimental harmonic response analysis [13], proved to be of utmost importance. The experimental activity consisted in hammer test of the cryomodule sub-assembly at an early assembly stage at which the internal parts, constituting the cold mass, were accessible allowing 20 triaxial accelerometers to be attached to the beam string. These accelerometers will remain embedded in the cryomodule, being available also during transportation, allowing further model validation at more advanced assembly stages. The comparison between the experimental modal analysis results obtained for the sub-assembly and the numerical results obtained for the corresponding multibody sub-model allowed to assess the reliability of the simulations and to get feedback on the effectiveness of the placement of the sensors in capturing the dynamic response of the system during transportation. Also, a refinement of the numerical model was performed to improve the matching between numerical and experimental data.

## 2. Sub-assembly description

The experimental activity was performed on a portion of the complete cryomodule, corresponding to the assembly stage at the first week of August 2019. At that assembly stage, the sub-assembly was composed by:

- strongback with mounting rods
- support posts
- lower portion of the thermal shield
- 8 cavities connected by their bellows (no couplers installed)
- 4 solenoids
- gate valves connected to temporary bracing (no end coups installed)

Two pictures of the studied assembly are shown in figure 1 and figure 2. The partially assembled Cryomodule was held in place employing four steel supports, each one connected to a rail by two linear bearings.



**Figure 1.** Partially assembled SSR1 Cryomodule.



**Figure 2.** Cavities, thermal shield and strongback accessible for sensor placement.

### **3. Hammer test description**

#### *3.1. Hitting locations*

A total number of 20 accelerometers were mounted on different components of the assembly (model EVAL-KXR94-2353 by Kionix Inc.). As an example, Figure shows one of these sensors fixed on a cavity.

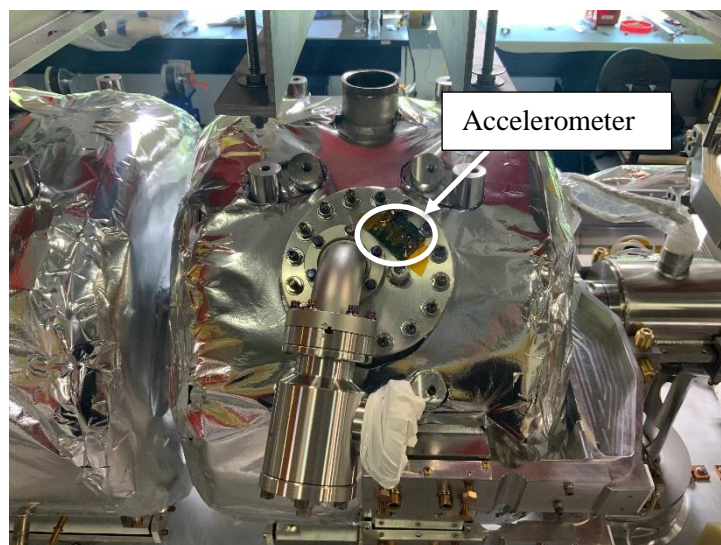


**Figure 3.** Accelerometer mounted on a cavity flange.

Each sensor can measure vibrations along 3 different axes, thus 60 acquisition channels were required to capture the response from all the accelerometers. An acquisition campaign was set up to collect all the data needed to perform the modal analysis of the cryomodule. Twenty hitting locations were identified on the main components of the structures (as shown in Figure ), which were hammered in both the longitudinal and transverse directions. During each acquisition, 12 vibration signals were recorded at once (because of a channel limitation of the data logger). Therefore, for each hitting position, 5 hits in the same location were needed to collect the response from all the accelerometers in the three directions, by switching the acquisition channels.

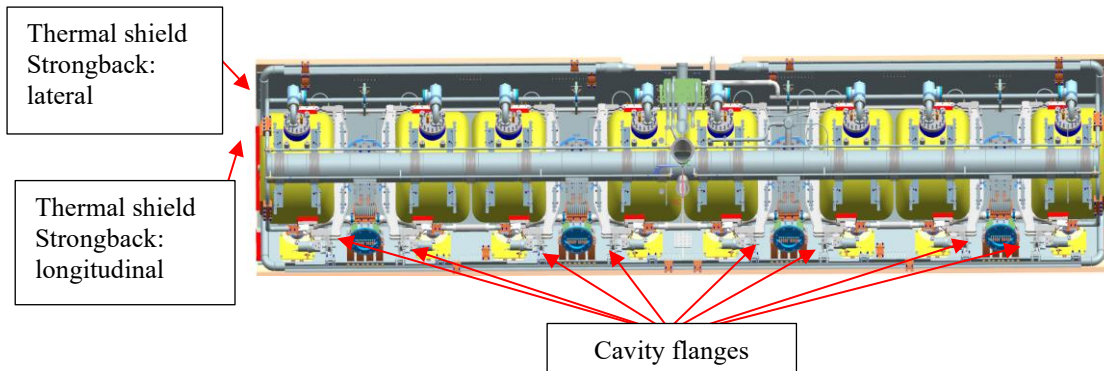


**Figure 4.** Hitting locations overview.

### 3.2. Accelerometer placement

**Errore. L'origine riferimento non è stata trovata.** shows the positions of the triaxial accelerometers on the assembly. Four sensors were placed on the strongback and the thermal shield respectively (8 accelerometers in total). Furthermore, every cavity was instrumented with one accelerometer (8 accelerometers in total) and four accelerometers were placed on two solenoids at two different locations.

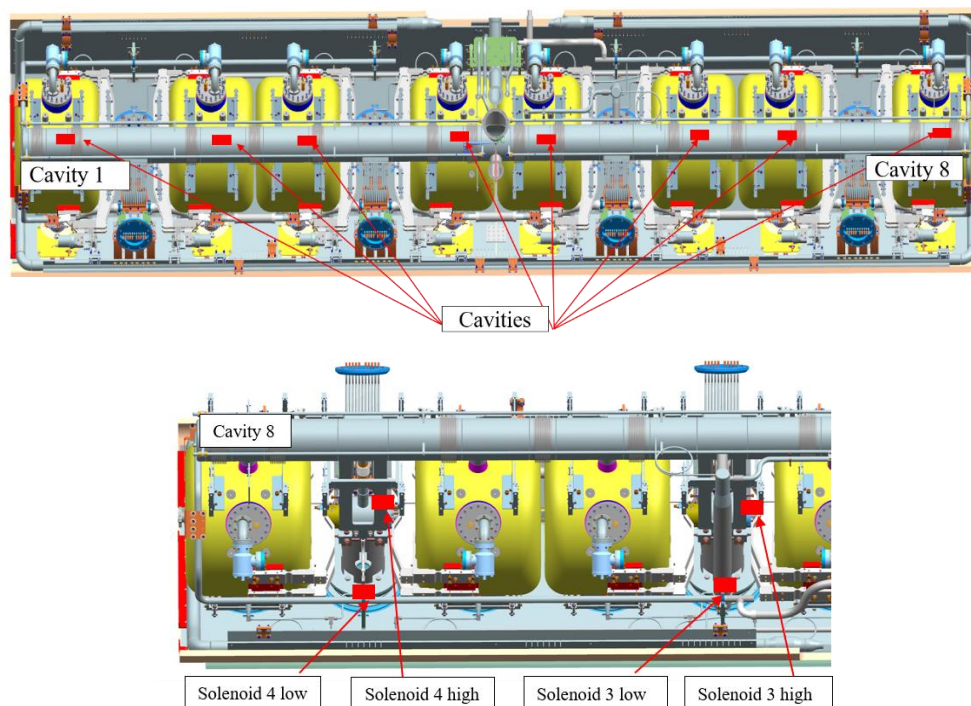


**Figure 5.** Accelerometer placement on the sub-assembly of the PIP-II proto SSR1 Cryomodule.

## 4. Experimental data analysis

### 4.1. Data processing

During the test, the structure was hit via an instrumented impact hammer and the acceleration at each sensor was measured. The subsequent step was the creation of a mathematical model capable of representing the natural modes of the structure by elaborating the acquired data. This process has been carried out by using the software Siemens - LMS Testlab.

The first step consisted in the creation of a simplified geometry of the Cryomodule, for graphical purposes. The modal shapes of the assembly can be visualized by importing the positions and the orientations of the accelerometers. In Figure each accelerometer is represented by a dot with its reference system. The colors distinguish the accelerometers depending on the components on which they are mounted. The experimental data recorded in the time domain (acquisition frequency 800 Hz) were then analyzed in the frequency domain. By combining the different measures related to each channel and for every hit, it was possible to reconstruct the dynamic response of the full system when subjected to the hammer excitations.

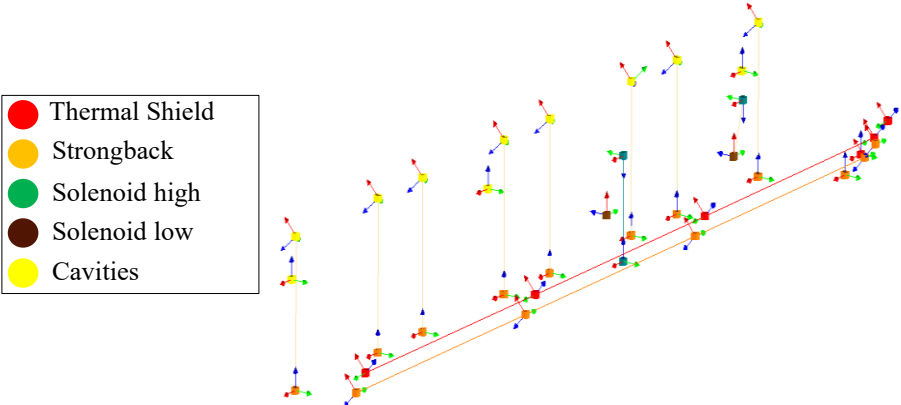


**Figure 6.** Overview of the geometry for the measurement points in Siemens - LMS Test.Lab.

The sum of the single frequency responses from each hit gives the overall Frequency Response Function (FRF) for the assembly. The FRF in the range of 0-40 Hz is shown in Figure . The elaboration of this FRF allowed identifying 23 modes, each one represented by a frequency and the corresponding mode shape.

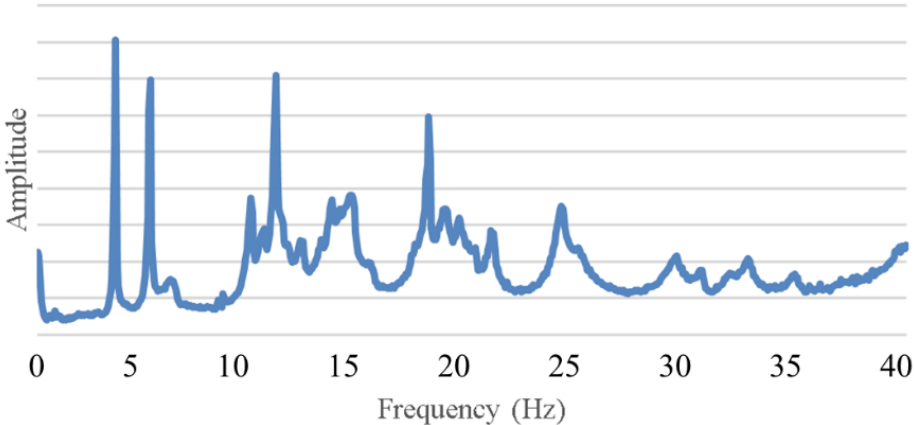


**Figure 7.** Overall FRF of the system in the range 0-40 Hz.

#### 4.2. Modal analysis results

The natural frequencies of the measured structure are listed in table 1 for the frequency range 0-40 Hz.

**Table 1.** Experimental natural frequencies of the system.

Mode N.	Exp. Peak (Hz)	Mode N.	Exp. Peak (Hz)
1	3.64	13	17.9
2	5.20	14	18.6
3	5.97	15	19.4
4	9.80	16	19.8
5	10.3	17	20.9
6	11.0	18	24.1
7	11.5	19	28.8
8	12.0	20	30.4
9	13.0	21	31.8
10	13.8	22	32.7
11	14.3	23	34.9
12	17.3		

At a glance, it is clear that the first three natural frequencies are appreciably lower than the others and well below the frequency value expected by the full-cryomodule numerical analysis, thus these modes appeared not related to the expected vibration of the cryomodule structure. To investigate more in-depth and to support this hypothesis, the mode shapes were plotted and these highlighted a rigid-body-motion of the sub-assembly associated with the first three natural frequencies. These low-frequency modes could then be ascribed to the vibration of the support system, which is mainly due to the compliance of the linear bearings which connect the supports and the rail. As an example, figure 8 shows the location of the undeformed accelerometers (grey) and the modal shape (coloured) associated with the 1st mode. As can be noted, all the measurement points rotate about the longitudinal axis, denoting a rigid-body roll motion. Conversely, figure 9 shows the same plot related to the 4th mode shape, in which the measurement points move out of phase with respect to each other, denoting a deformative mode.

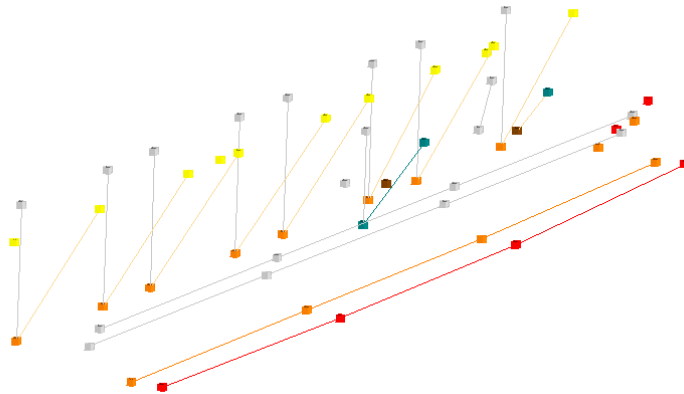


**Figure 8.** Undeformed (grey) and deformed (coloured) geometry of the accelerometers relative to the 1st mode of vibration.

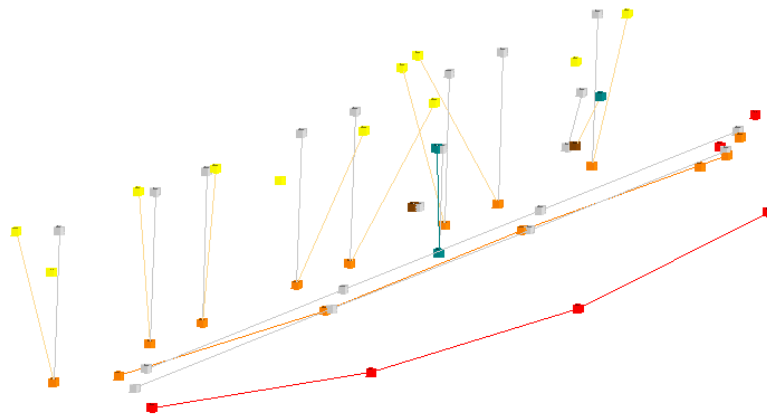


**Figure 9.** Undeformed (grey) and deformed (coloured) geometry of the accelerometers relative to the 4th mode of vibration.

## 5. Data comparison with model prediction

To reproduce the behavior of the system in the range of frequencies of interest, a numerical model was developed corresponding to the measured sub-assembly. The setup of the model followed the assumptions and the guidelines described in [11]. Different modelling strategies were tested concerning two critical aspects: the connection of the cryomodule to the ground and the connection of different components of the cold mass. The comparison between modal experimental and numerical data allowed the evaluation of the performances of each strategy, to determine which one is more suitable for future analysis.

### 5.1. Numerical model with spherical joints

The first approach consisted in modelling the connection of the assembly to the ground through spherical joints at the feet of the strongback (8 spherical joints in total), as shown in figure 10. The corresponding numerical natural frequencies are reported in table 2.

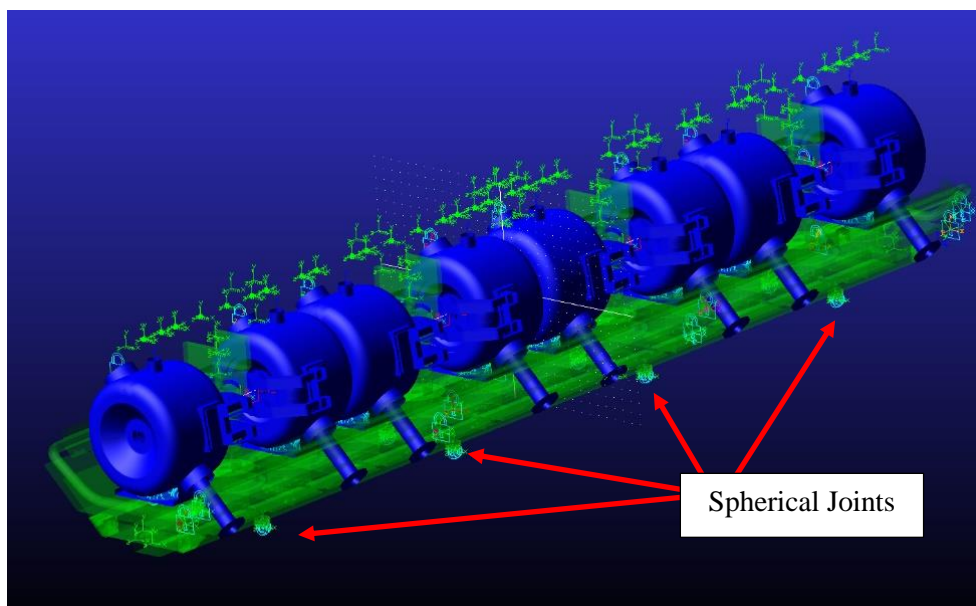


**Figure 10.** Preliminary model with spherical joints at the feet.

A comparison between table 1 and table 2 highlights a poor correlation between this model and the experimental results. Indeed, the numerical frequencies are generally higher than the experimental ones, showing that the simulated constraints overestimate the frequencies of the actual cryomodule response.

**Table 2.** Natural frequencies for the model with spherical joints.

Mode N.	Num. Peak (Hz)	Mode N.	Num. Peak (Hz)
1	13.5	9	23.0
2	14.9	10	24.0
3	17.8	11	24.9
4	18.3	12	25.3
5	18.6	13	25.4
6	18.7	14	25.8
7	21.2	15	25.9
8	22.7	16	26.0

*5.2. Numerical model with support system*

To improve the accuracy of the numerical model, a more realistic representation of the support system was implemented. Simplified geometry of the supports was introduced in the model. Additionally, the compliance of the mounting bearings was simulated through 3 lumped stiffnesses (simulated as linear springs along three directions), whose stiffness was assessed and tuned to obtain a satisfactory matching with experimental results. The modified model is shown in figure 11. The simulation results are reported in table 3.

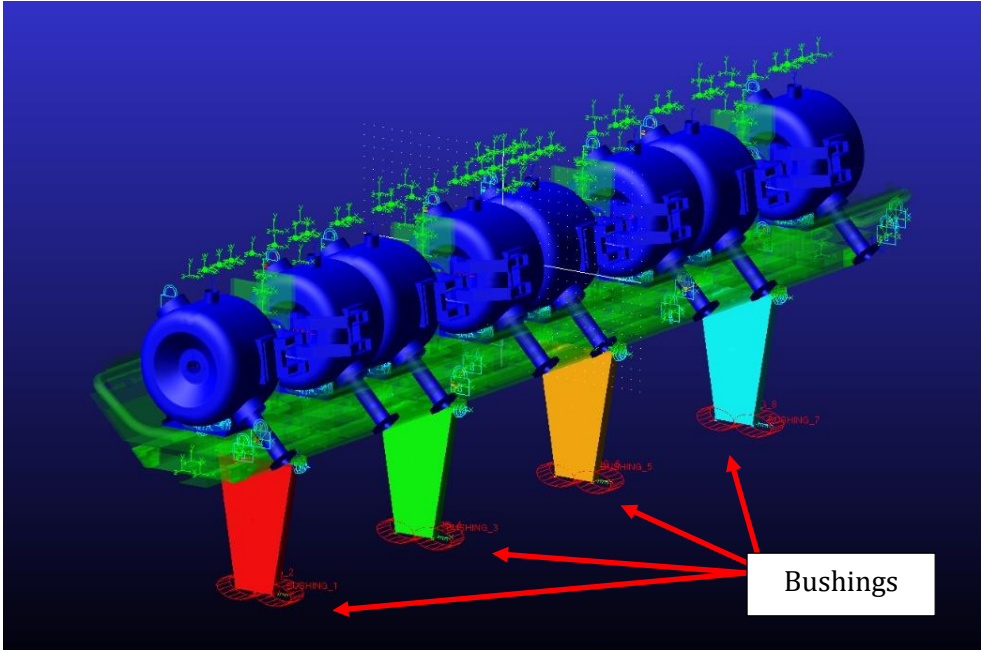


**Figure 1.** Updated model with compliant bushings at the base of the supports.



**Table 3.** Natural frequencies for the model with bushings.

Mode N.	Num. Peak (Hz)	Mode N.	Num. Peak (Hz)
1	3.58	9	21.7
2	4.18	10	23.0
3	5.47	11	23.4
4	14.4	12	24.8
5	15.6	13	24.9
6	16.8	14	25.2
7	17.9	15	25.7
8	20.7	16	26.0

### 5.3. Discussion

The comparison between the updated model natural frequencies and the experimental results is reported in table 4.

**Table 4.** Comparison between experimental and the numerical frequencies.

Mode N.	Exp. (Hz)	Num. (Hz)	Mode N.	Exp. (Hz)	Num. (Hz)
1	3.64	3.58	10	13.8	23.0
2	5.20	4.18	11	14.3	23.4
3	5.97	5.47	12	17.3	24.8
4	9.80	14.4	13	17.9	24.9
5	10,3	15.6	14	18.6	25.2
6	11.0	16.8	15	19.4	25.7
7	11.5	17.9	16	19.8	26.0
8	12.0	20.7	17	20.9	26.5
9	13.0	21.7	18	24.1	26.6

The new numerical model matches better the experimental frequencies for the first three rigid-body modes. However, there is still a discrepancy between experimental and numerical results concerning the deformative modes. This mismatch can be ascribed to many uncertainties in the model, such as non-rigid connections and constraints among the various components at bolted joints and uncertainties about the masses and inertia of the components of the real structure.

Finally, the modal shapes were extracted from both experimental and numerical results. Thus, it was possible to compute the Modal Assurance Criterion (MAC) [14] between these two sets of mode shapes, which allows comparing the shapes of the two-mode sets. High MAC values denote a good shape matching, while low MAC values denote a poor shape matching. The MAC values for the studied assembly are reported in figure 12.

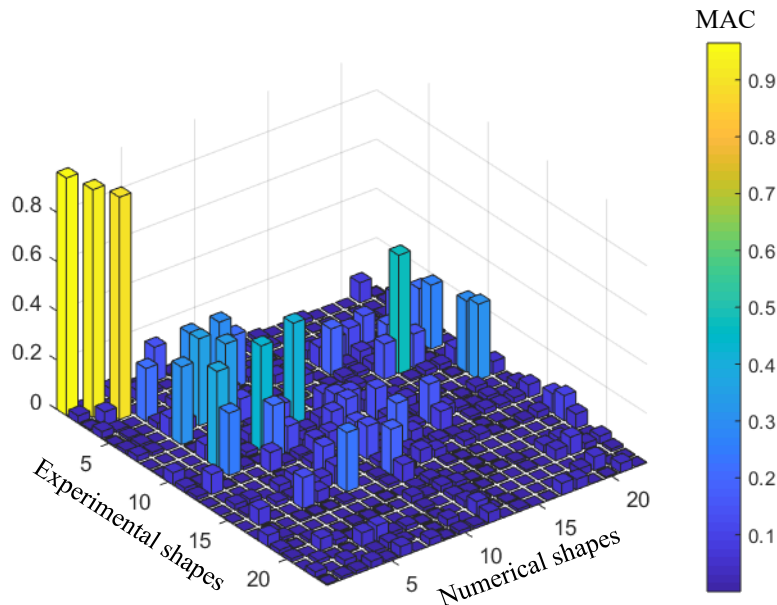


**Figure 2.** MAC matrix between numerical and experimental modes.

The developed numerical model successfully reproduces the natural frequencies as well as the modal shapes of the real system for the first three rigid modes. On the other hand, the matching of the deformative modes still needs to be enhanced by tuning other model parameters, such as component connection stiffnesses and inertia properties.

## 6. Conclusions

This activity aimed to experimentally determine the first modes of vibration of the SSR1 Cryomodule. The task consisted of two different phases. In the first phase, experimental modal analysis has been carried out, through a series of accelerometers placed on the key components of the assembly. The dynamic response of the system has been recorded by exciting the structure with an instrumented hammer. In the second phase, the data acquired have been analyzed in the frequency domain to determine the natural frequencies of the system. The experimental results were compared with the numerical results, allowing the tuning of some parameters to obtain a better match at least for the first modes. The presented results confirmed the possibility to enhance the matching between experimental and numerical results by tuning model parameters, such as connection stiffnesses and inertia properties. In future developments, optimization of these parameters will be carried out for the full assembly, to improve the model reliability and to draw more precise guidelines for modelling similar assemblies.

## References

- [1] Wu G 2019 SRF cryomodules for PIP-II at Fermilab. Presented at: 19th International Conference RF Superconductivity, SRF 19; June 30 – July 5; Dresden, Germany.
- [2] Barzi E, Gallo G, Neri P 2012 FEM analysis of Nb-Sn Rutherford-Type Cables. *IEEE Trans. Appl. Supercond.*; **22**(3).
- [3] Roger V, Cheban S, Nicol T, Orlov Y, Passarelli D, Vecchiolla P 2018 Design update of the SSR1 cryomodule for PIP-II project. Proceedings of the 9th International Particle Accelerator Conference IPAC 18; Vancouver, Canada.
- [4] Passarelli D, Wands R, Merio M, Ristori L 2016 Methodology for the structural design of single spoke accelerating cavities at Fermilab. *Nucl. Instrum. Methods Phys. Res. A* **834**: 1–9.
- [5] Conway Z, Barcikowski A, Cherry G, Fischer R, Guilfoyle B, Hopper C, et al. 2016 Progress Towards a 2.0 K Half-Wave Resonator Cryomodule for Fermilab's PIP-II Project. Part of:

- Proceedings of the 28th Linear Accelerator Conference, LINAC 2016.
- [6] Kim S, Conway Z, Kelly M, Ostroumov P, Gerbick S, Reid T, et al. 2015 Preservation of Quality Factor of Half Wave Resonator during Quenching in the presence of Solenoid Field. Part of: Proceedings, 6th International Particle Accelerator Conference, IPAC 2015.
  - [7] Li J, Harms ER, Hocker A, Khabiboulline TN, Solyak N, Wong T 2011 Development and Integration Testing of a Power Coupler for a 3.9-GHz Superconducting Multicell Cavity Resonator. *IEEE Trans. Appl. Supercond.* **21**(1):21–26.
  - [8] Whitlatch T, Curtis C, Daly E, Graves C, Henry J, Matsumoto K, et al. 2001 Shipping and alignment for the SNS cryomodule. Published in: PACS2001. Proceedings of the 2001 Particle Accelerator Conference; Chicago, IL, USA.
  - [9] McGee M, Bocean V, Grimm C, Schappert W 2008 Transatlantic transport of Fermilab 3.9 GHz cryomodule for TTF/FLASH to DESY. Part of: Particle accelerator. Proceedings, 11<sup>th</sup> European Conference, EPAC 2008; Genoa, Italy.
  - [10] Bertini L, Bucchi F, Monelli BD, Neri P 2018 Development of a simplified model for the vibration analysis of lawn mowers. *Procedia Struct. Integrity.* **8**: 509-16.
  - [11] Neri P, Bucchi F, Passarelli D 2020 A multilevel finite element-multibody approach to design the suspension system for the road transportation of SSR1 cryomodule. *J. Transp. Eng.* **2**.
  - [12] Bertini L, Neri P, Santus C, Guglielmo A 2017 Automated Experimental Modal Analysis of Bladed Wheels with an Anthropomorphic Robotic Station. *Exp. Mech.* **57**:273-85.
  - [13] Bertini L, Neri P, Santus C, Guglielmo A 2017 One Exciter per Sector Test Bench for Bladed Wheels Harmonic Response Analysis. Part of: Proceedings of ASME Turbo Expo 2017: Turbomachinery Technical Conference and Exposition; Charlotte, NC, USA.
  - [14] Bertini L, Neri P, Santus C, Guglielmo A 2014 Robot Assisted Modal Analysis on a Stationary Bladed Wheel. Part of: Proceedings of the ASME 2014 12th Biennial Conference on Engineering Systems Design and Analysis; Copenhagen, Denmark.